VILNIUS TECH
Vilnius Gediminas Technical University

Geodesy and Cartography
ISSN 2029-6991 / eISSN 2029-7009
2023 Volume 49 Issue 2: 76–87
https://doi.org/10.3846/gac.2023.16990

UDC 528.8.042

ANALYSIS OF TWO-OPTION INTEGRATION OF UNMANNED AERIAL VEHICLE AND TERRESTRIAL LASER SCANNING DATA FOR HISTORICAL ARCHITECTURE INVENTORY

Szymon SOBURA[1*], Kamil BACHARZ[2], Grzegorz GRANEK[1]

[1]*Department of Geodesy and Geomatics, Faculty of Environmental, Geodesy and Renewable Energy, Kielce University of Technology, Kielce, Poland*
[2]*Department of Concrete and Geotechnical Engineering, Faculty of Civil Engineering and Architecture, Kielce University of Technology, Kielce, Poland*

Received 16 May 2022; accepted 16 May 2023

Abstract. The 3D reconstruction of historical and cultural heritage monuments is a procedure recommended by the UNESCO World Heritage Institution since 1985. It is crucial when conserving monuments and creating digital twins. Current 3D reconstruction techniques using digital images and terrestrial laser scanning (TLS) data are considered as cost-effective and efficient methods for the production of high-quality digital 3D models. In the presented study, laser scanning and close-range photogrammetry techniques and images taken by a low-cost unmanned aerial vehicle (UAV) were applied to quickly and completely acquire the point cloud and texture of a historic church in Poland. The aim of this study was to evaluate two options for integrating TLS and UAV data, using ground control points (GCP) measured by two independent techniques: tachymetry and laser scanning. The study shows that the 3D model created based on ground control points acquired by the laser scanning technique has a mean square error $RMSE_{XYZ}$ = 2.5 cm on the check points. The result obtained is not much larger than the second variant of data integration, for which $RMSE_{XYZ}$ = 1.7 cm. Thus, the TLS method was positively evaluated as a GCP measurement technique for the integration of UAV and TLS data and the creation of cartometric 3D models of religious buildings.

Keywords: TLS, UAV, close-range photogrammetry, data integration, digital twins, low-cost drone.

Introduction

The maintenance of cultural heritage documentation and conservation resources is increasingly carried out using 3D products. This is reflected in work related to conservation, as-built documentation, reconstruction and the creation of digital museum exhibitions (Xu et al., 2014; Mikoláš et al., 2014; Federman et al., 2018). Among the many data acquisition techniques in 3D space, we can distinguish methods based on digital images and laser scanning (Hejmanowska et al., 2017). Both techniques have advantages and disadvantages, while synthetically they allow one to achieve very good effects and accuracy in the process of creating inventory documentation of monuments. According to (Liang et al., 2018), the integration of both techniques gives all the better results (compared to the situation where only one technique is used) when the object under study has a complex geometry or is difficult to measure with traditional methods.

One of the challenges of aerial data acquisition for 3D visualisation is the choice of flying platform, data processing and data quality. A point cloud created from photographs is characterised by a large amount of measurement noise. This noise can be reduced to some extent during post-processing, but not eliminated entirely. The advantage of UAV (Unmanned Aerial Vehicle) technology in the context of 3D model creation is: low cost of data acquisition and the equipment itself, the possibility of creating realistic textures and reaching places difficult to access e.g. roofs of buildings or higher floors of buildings. For Terrestrial Laser Scanning (TLS) measurements, a common limitation of the technology is the high cost of the equipment. In addition, the internal camera built in laser scanners can be sensitive to lighting changes and overexposure, which limits the creation of photorealistic textures for the reconstruction of cultural and historical monuments. However, a point cloud derived from TLS is less noisy and the accuracy of determining individual

*Corresponding author. E-mail: *ssobura@tu.kielce.pl*

measurement points is higher than a point cloud created from photographs. Moreover, the advantage of laser scanning over classical photogrammetry is the possibility to take several samples of surface types that are in the line of sight of the laser beam, until the impermeable surface prevents further penetration of the laser energy (Šašak et al., 2019).

The presented data acquisition techniques complement each other and thus overcome the weaknesses of each of them. For this reason, in many works (Escarcena et al., 2011; Xu et al., 2014; Reiss et al., 2016), authors recommend the integration of different sensors and techniques to create geometrically accurate and realistic 3D models.

Current 3D reconstruction techniques using a digital image, according to (Escarcena et al., 2011; Xu et al., 2014), are considered to be cost-effective and efficient methods for producing high-quality digital 3D models. Together with the development of image matching techniques and algorithms, the modelling results are becoming more precise (Gradka et al., 2019). For spatially complex objects, they require digital images with high forward and side overlap. Using the SfM (structure from motion) method implemented in many photogrammetric software (e.g. Agisoft Metashape, Pix4D), it is possible to acquire the geometry of the reconstructed scene by processing multiple images simultaneously. Some of the steps are fully automated, which speeds up the process of creating a cartometric 3D model – especially when using converging images (Reiss et al., 2016).

UAV platforms equipped with an optical camera and GNSS systems (Global Navigation Satellite Systems), allow to solve many problems of close-range photogrammetry concerning, among others, determining approximations of external orientation elements of images or reaching places difficult to access (e.g. roofs of buildings) (Federman et al., 2018). A weakness of TLS scanning is the inability to acquire information about building roofs, which can be compensated by UAV technology (Xu et al., 2014; Bieda et al., 2020). Moreover, UAV technology has recently become an interesting complement to TLS, by generating point clouds with not much worse accuracy than TLS (Šašak et al., 2019). The large amount of information contained in digital images from UAVs allows not only to create cartometric products in the form of orthophotos and 3D models, but also to help the economic sector make smarter decisions (Gbopa et al., 2021; Karabin et al., 2021).

In the presented study, TLS and UAV techniques were used to quickly and completely acquire the point cloud and texture of a historic church in Poland. The purpose of the study was to assess the impact of different ways of integrating UAV and TLS data on the quality of the resulting 3D model. The steps taken to achieve the objective were to perform a scan around the research object and to perform a photogrammetric flight with a UAV platform. Two variants of spatial data fusion were presented in this paper: a) using precisely measured photogrammetric reference points (ground control points) with a tachymeter and b) using established photogrammetric reference points measured by laser scanning. Both methods differed in terms of accuracy and labour consumption. The analysis of the two variants presented was to help optimise the process of integration of UAV and TLS data for future documentation of sacral objects and to answer the question if scanning of stabilised ground control points (chequerboard targets for UAV flights) allows to obtain comparable accuracy of 3D models as in the case of determining the coordinates of the geodetic network with a precise total station.

1. Literature review

3D reconstruction of historical heritage monuments is a procedure recommended by the UNESCO World Heritage Institution since 1985 (Xu et al., 2014). It is crucial during the preservation of monuments and the creation of digital twins. In this way, in the event of a disaster related to the damage or destruction of a monument, it is possible to partially or fully rebuild it for future generations. Furthermore, the paper (Jo & Hong, 2019) highlights that the acquisition of full geospatial information is important for the systematic management, monitoring and response to possible deformations of a monument. Preventive measures in the form of creating full digital documentation of national heritage monuments are increasingly actively promoted worldwide (Mikoláš et al., 2014; Reiss et al., 2016; Hejmanowska et al., 2017), which further highlights the importance of this issue.

For 3D reconstruction and visualisation of cultural heritage objects, TLS systems are frequently used as a solution. Laser scanning is one of the many methods currently used to perform a wide range of tasks related to, among others: inventory of urban spaces (Esmer et al., 2019), building and engineering objects, including objects of historical significance (Ramondino, 2011) and assessment of their condition, including deformation studies (Chow, 2014; Lipiceki et al., 2017; Sztubecki et al., 2018). The TLS measurement method allows quick reconstruction of monument geometry with high accuracy of detail representation (Jo & Hong, 2019). TLS captures both spatial point data and radiometric information in the form of point colour and reflection intensity. Based on fast measurements of distance and horizontal and vertical angles, a point cloud is determined. It is a reprocessed representation of the object under study in the instrument's local coordinate system. The huge amount of captured data, up to several hundred thousand points measured per second, allows the generation of very detailed and reliable surface models. On the other hand, such a huge data set may pose a problem in post-processing, which results in filtering and often removal of data fragments at the post-processing stage (Escarcena et al., 2011; Róg & Rzonca, 2021).

Many cartometric products are now created using photogrammetric methods and images acquired from aircraft or UAVs (Cienciała, 2018; Gradka et al., 2019; Gbopa et al., 2021). Aerial images have a great potential for information, and the possibility of obtaining information in

areas difficult to access remotely supports their increasing use (Mikrut et al., 2013; Karabin et al., 2021). The photogrammetric documentation performed allows for a complete assessment of the condition of the studied object and a comparison of periodic results. They also can be useful for monitoring a monument subject to deformation (Mikoláš et al., 2014).

The use of measurement techniques providing 3D data, favours 3D modelling and the creation of high-resolution orthomosaics for cultural heritage documentation. Dense point clouds make it possible to select the required cross-section of a research object and create a 2D line drawing with measures for detailed inventory based on it. According to (Liang et al., 2018), this way of documenting the results is to some extent more relevant and understandable than the created 3D model. Although the 3D model is cartometric, conducting spatial measurements is difficult and requires specialised software.

2. Study area

The object of study was a Roman Catholic church listed in the Polish Monuments Register and located in Chełmce, 14 km north-west of the city of Kielce. The detailed location of the site is shown in Figure 1. The church is situated on top of a hill called Góra Plebańska. The temple was built in the mid-17th century and is orientated and consists of a three-bay nave. The presbytery is adjoined by twin chapels of St George and St Nicholas. A characteristic element of the historic church is a lofty tower with a quadrilateral base in the lower part and an octagon base, in the upper part, covered with a three-storey helmet with a spire (Zespół kościoła parafialnego…, n.d.). The building was erected in the early Baroque style. The church analysed in this study is located on an elevation, surrounded on all sides by steep escarpments, which means that the research object is located in the zone of potential influence of vertical movements of the escarpments. Thus, conducting cyclic observations of the church condition may lead to monitoring of this monument for deformations, which may eventually lead to damage including e.g., frequent in these cases, cracks on the facades.

The main reason for choosing the object presented for the investigation was the preservation of the reported cracks in the church façade. Due to the large size of the object, it was decided to conduct inventory activities with the use of UAV and TLS technologies in order to create a digital 3D model as a basis for further digital

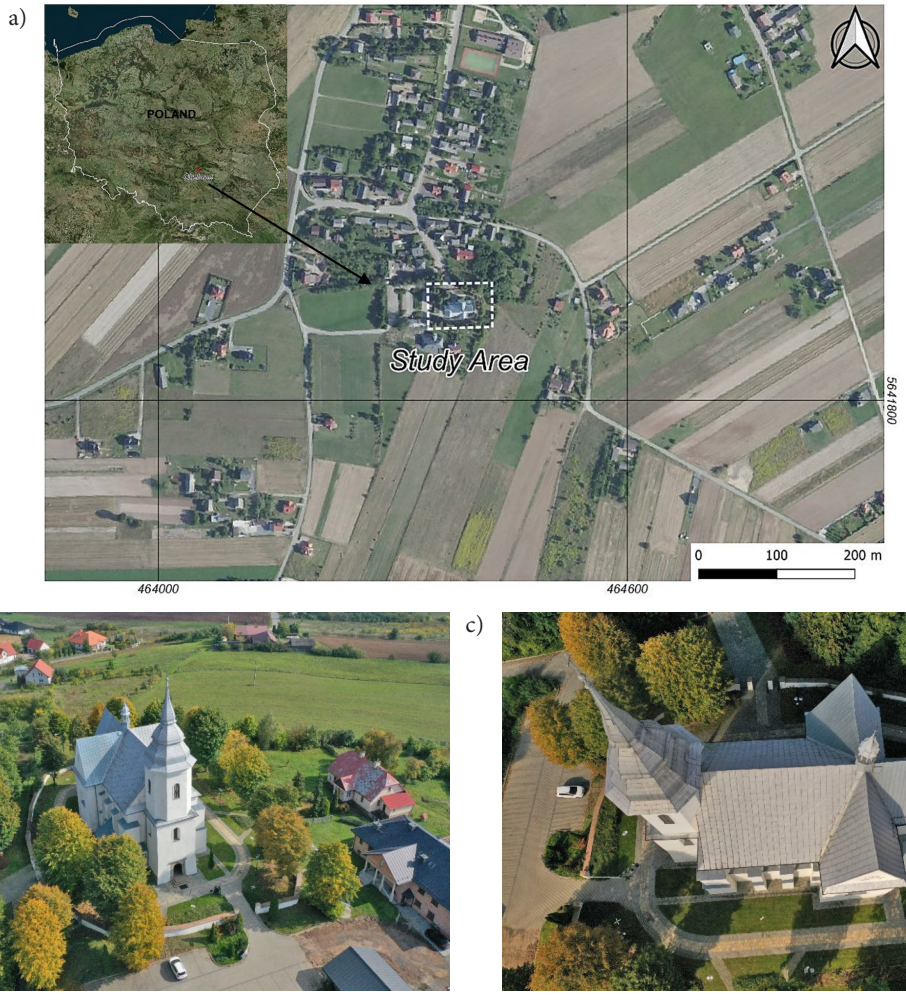

Figure 1. Historical church in Chelmce: a – location of research object on the background of Poland (coordinates in UTM system, 34N zone (WGS84)); b – view of church from west; c – view of church from south

documentation of the church object. Thus, the research presented was also practical and the results obtained could be implemented in the assessment of the building in terms of planned conservation.

3. Methodology of the work performed

The chapter describes the data acquisition methodology for creating a 3D model of a religious object in Poland, together with the problem of integrating data from various sensors. The whole work can be divided into four main stages:

- stabilisation and measurement of marked ground control points,
- spherical targets placement and laser scanning,
- UAV flight,
- integration of TLS and UAV point clouds.

The aim of the work was to create two 3D models, which were created after data integration by using ground-based checkerboard targets measured by tacheometry or laser scanning. The resulting 3D models should be checked for both quality and accuracy of geometry reproduction with the technical condition. Due to the lack of current regulations in Poland on the accuracy of surveying historic buildings, it is the client who imposes the accuracy of the resulting study. In the present study, it has been assumed that the results obtained will allow the 3D measurements to be made with an accuracy of less than 5 cm. A detailed schematic of the data acquisition and post-processing steps, as well as the integration of the TLS and UAV results, is presented in Figure 2.

3.1. Tachymeter measurement of control points

During the planning of the geodetic network for the present study, several aspects were taken into account that could influence the accuracy and usability at a later stage of data integration. A group of points was designed in a configuration ensuring coverage of the entire object, taking into account their visibility for the scanner and in the photogrammetric images. Ultimately, the obtained coordinates were also to guarantee geo-location in accordance with the national coordinate system PL-2000 (EPSG:2178). It was assumed that the ground control points should be characterised by errors smaller than those for a typical single point from laser scanning (2–10 mm), in order to minimise losses resulting from merging adjacent data sets.

Taking this into account, it was decided to carry out the measurement in a geodetic network system with over-abundant observations. A Topcon QS1 robotic total station was used, with a direction accuracy of m_k = ±1" and a distance determination error of m_d = ±1 ppm. The servomotors present in the instrument improved the measurements in full-angle repetition. The centres of chequerboard discs placed on the ground were measured. A miniprism was used at the lowest possible target height.

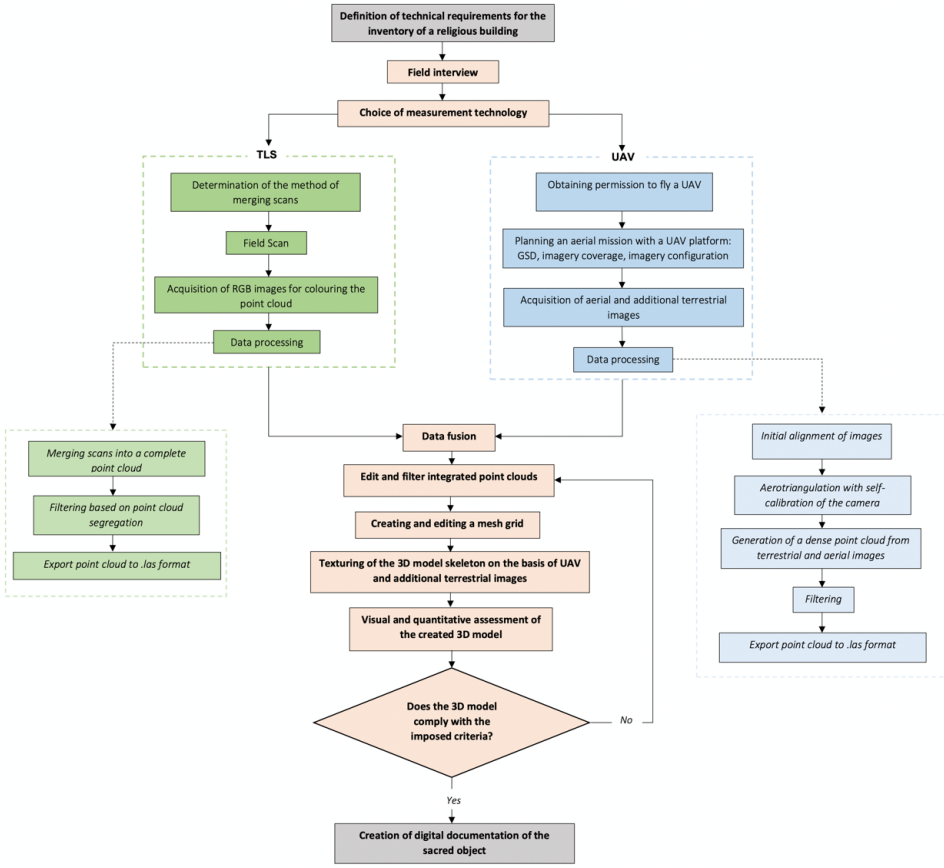

Figure 2. Workflow of integration of UAV and TLS data (source: own study based on Jo & Hong, 2019)

a) b)

Figure 3. Equipment used during measurements: laser scanner Faro Focus 150S (left), spherical patterns (right) and signalled ground control points (GCP) in the form of chequerboard targets

In order to give the desired geo-location, several points were measured using the GNSS-RTN method in the national spatial reference system. For the set of measurement data, an exact parametric least squares adjustment was made using the free method, assuming the only crucial conditions for obtaining correct location and orientation in space, i.e. one fixed point and pseudo-observation of azimuth on the basis of the quoted satellite measurements. Due to the small area of the imaging, corrections due to the reference system were excluded. As a result, coordinates in the desired datum were obtained with improved accuracy, which is characteristic for tacheometric measurements. The results were processed using the least squares method. The accuracy of individual measurement points of < 3 mm was achieved for a confidence level of one standard deviation. In the alignment process, the standard deviation parameter m_0 = 0.78 and the individual observations received corrections no greater than the accepted instrumental errors. This confirms the correct measurement and data processing. The accuracy of the prepared network meets the assumptions of the conducted research and is consistent with the experience of other authors (Granek et al., 2020).

3.2. Laser scanning survey (TLS)

Acquiring point clouds using the TLS method for the purpose of creating 3D models, brings with it a variety of issues related to efficient and effective measurement sessions (Hlotov & Marusazh, 2019; Róg & Rzonca, 2021). These will include ensuring coverage for the entire project, controlling the resolution range for all scan elements, or maintaining similar, homogeneous accuracy levels for the resulting point cloud. To obtain the desired results, data logging was performed from multiple sites, often with repeated coverage. After combining the scans, a homogeneous point cloud with correct mutual orientation was obtained.

In this study, the Faro Focus 150S scanner (FARO, n.d.), which is the equipment of Kielce University of Technology, was chosen to carry out the inventory of the church object. This device enables scanning indoors and outdoors under different lighting conditions within a radius of up to 150 m. The maximum range can be obtained when scanning surfaces with a reflectivity of 10 to 90%, while with a reflectivity of 2 to 10% the measurement range drops to 50 m.

The Faro Focus 150S enables scanning accuracy of up to 1 mm with a measurement tolerance of 0.2 mm, at distances of 10 m to 25 m and for surfaces with a reflectivity of about 90%. When acquiring scans on the outside of structures, the distances between the measured points were at the level of 12.3 mm (at a distance of 10 m to the measuring object). In the case of scans taken in locations with varying lighting conditions, in addition to averaging the illuminated area, the HDR function (High Dynamic Range) was used to obtain a coloured point cloud of better quality. During the work, spheres and chequerboard targets (Figure 3) were deployed for subsequent post-processing of the data. As a result of the survey work, 16 scans were taken around the survey object.

The merging of the working scans was carried out using the SCENE software. The process of registering the individual scans itself was carried out using the two main joining methods available in the SCENE software, i.e. Cloud to Cloud and Top View Based. In the case of unsatisfactory joining accuracy of selected scans, an additional method of manual joining of scans was used. For this purpose, surfaces and common elements on the merged scans were manually indicated. Spherical patterns placed in areas of increased scanning difficulty were also used. A mean square error of $RMSE_{XYZ}$ > 20 mm and an overlap of less than 10% between the scans were considered as values that indicate the need to improve the merging of the individual scans. The end result was an average fit error for all scans of 2.5 mm with a maximum local error of 8.4 mm. The resulting merged file was then processed into a homogeneous point cloud, resulting in a resampled test object of more than 254 million points.

3.3. Photogrammetric flight

Before an UAV flight, the status of airspace activity over the study area presented in Figure 1 was checked using a teleinformatic system recommended by the Polish PANSA service. The UAV flight took place in the G class airspace.

An amateur unmanned aerial vehicle, Mavic 2 Pro, was used to acquire aerial images, and its specifications are presented in Table 1.

Table 1. Specifications of the Mavic 2 Pro drone used in the study

Weight	0.91 kg
Camera matrix	1" CMOS, 20 MP
Lens	FOV: 83° (25mm); 48° (48mm) eqivalent to format 48 mm, f/2.8
Flight time on one battery	~24 minutes
IP tightness standards	No
RTK/RTN corrections	No

During the UAV flight, vertical and oblique images were acquired, with the aim of fully representing the object studied and to make visible all the details of the cultural monument. This approach is consistent with the experience of other researchers (Puniach et al., 2018; Federman et al., 2018; Pyka et al., 2020). The forward and cross overlap value of the images was set at 70%. A total of 180 aerial images with an average terrain pixel of 1.5 cm/pix were acquired. In addition, a series of images from below were taken for objects not visible from above, e.g. gates, windows, and the underside of the roof projecting beyond the building wall. The quality of UAV images was checked by determining the QI (Quality Image) parameter. Its value for all images was within the range (0.85–0.90), which confirmed that the images are sharp and suitable for further processing.

The process of aligning the images with simultaneous camera self-calibration was performed in Agisoft Metashape software based on the bundle method, which allows for accurate calculation of the external orientation elements of the images and minimisation of projection errors (Xu et al., 2014). Carrying out the digital camera calibration process involving the determination of the camera's internal orientation elements, according to (Mikoláš et al., 2014), is a necessary step for the correct reconstruction of the geometry of the studied object. The optical camera calibration process includes defining the geometry of the sensor model in the form of the camera constant (ck), the coordinates of the principal point and the image errors modelling distortion (Kapica et al., 2013; Sobura, 2022). Camera self-calibration is based on the simultaneous solution of photogrammetric intersection and resection indentation and uses the colinearity equation model in doing so. In this study, the calibration of the UAV camera was based on self-calibration during the survey process using ground control points (GCPs) measured in the field.

After aerotriangulation with self-calibration of the UAV camera, a dense point cloud was generated in Agisoft Metashape software. Detailed filtering of the UAV point cloud was performed in Cloud Compare software. After filtering, the point cloud was checked for missing spatial information. Missing points were observed around the folds of the base of the church and on the walls of its tower.

3.4. Integration of TLS and UAV data

Sacred objects usually have a complex geometric structure, therefore the documentation of the shape of such a monument by laser scanning alone is, according to (Jo & Hong, 2019), difficult and in places impossible (e.g. on roofs and towers). Furthermore, the acquired TLS data have a variable sampling density depending on the distance of the scanner to the object being measured. For very tall objects (e.g. tall towers), this can lead to a sparse point cloud at the edge of the scan and result in an unrepresentative geometry for object reconstruction. The inaccessibility of such locations to TLS technology can be eliminated by UAV technology and multidirectional data integration.

One of the most accurate, yet highly efficient methods of combining scans is to place spherical marks on adjacent images (Reshetyuk, 2009; Cox, 2015; Kowalska & Zaczek-Peplinska, 2018). Unfortunately, for spatially extensive objects that require scans from multiple sites, this method is insufficient. Furthermore, in this study, the final model is the result of the integration of TLS scanning technology with photogrammetric methods based on UAV images, which further forces the introduction of checkboard targets. For the purposes of this study, a solution was proposed to combine all data sets in a way that

a) b)

Figure 4. Visualisation of acquired point clouds based on: a – TLS; b – UAV

ensures accurate control and also gives the whole a proper geolocation. For this purpose, a measurement network of points was designed in the form of a geodetic control network designed for high precision.

Both series of independently acquired data contained local voids or too sparse coverage for full reconstruction of the object, as shown in Figure 4. For the TLS data, large data voids were observed in the upper part of the research object: around the tower and on the roofs. On the contrary, the point cloud created from the UAV images was characterised by a large amount of noise around the edges of the building and the roof, and missing data at the base of the church. For this reason, it was assumed that the integration of TLS and UAV data is necessary for the correct reconstruction of the geometry of the studied church object, which confirms the experience of other authors (Bieda et al., 2020).

Point clouds independently acquired from two different sensors were integrated with each other in the Cloud Compare software. A prerequisite for data integration was to have both point clouds in the same coordinate system. In the presented studies, point clouds were transformed to a common coordinate system for two analysis variants: a) for the national coordinate system from the total station measurement, b) for the local system determined by the scanner.

The first fusion of TLS and UAV data was performed based on point cloud transformations from the TLS to the state coordinate system 2000 zone 7 (EPSG: 2178). The spatial coordinates of three terrestrial chequerboard targets, measured by tacheometry, were used for the transformation. For the first variant, the UAV images were processed in the same coordinate system. Thus, by importing both point clouds (from TLS and UAV measurements) into Cloud Compare, it was possible to display them in the same region and obtain faster convergence of calculations.

The second option involved processing the UAV images in the coordinate system of the point cloud from the TLS (local laser scanner system). As in the first option, the point cloud generated from the UAV images was matched with the point cloud from TLS in the Cloud Compare software.

After integration and filtering, the resulting point cloud was triangulated to create a triangle mesh in Agisoft Metashape software. The option of generating a mesh for an object with spatially varying geometry was selected (option: arbitrary). The mesh was checked for holes and incorrect interpolation and the identified errors were manually corrected. In the final stage, the mesh model was smoothed and cleaned using the Refine Mesh function.

The final step in creating the 3D model was to create a realistic texture. In photogrammetric work, texturing is mainly used to show a virtual model of inventoried 3D objects aiming to reproduce their real appearance as closely as possible (Tokarczyk et al., 2012). In this study, the "adaptive orthophoto" option and a texture resolution of 8k were chosen, which proved to be suitable for texturing the 3D model analysed in the paper. The entire surface of the object when texturing with the "adaptive orthophoto" option, is divided into a series of horizontal and vertical segments, which allows for an accurate representation of the texture and colour of the object. The occurrence of errors at this stage can only be caused by incorrect mesh generation (Gradka et al., 2019). Texturing of the 3D model in its lower parts and places difficult to see from the upper level (e.g., under the roof) was performed based on complementary images acquired with a drone at low level, holding the drone in the hand, and treating it with a terrestrial camera. The images acquired in this way were resolved into a single image network together with images acquired during the UAV photogrammetric flight.

4. Results

The following chapter presents the results of the integration of TLS and UAV data in the form of 3D models, for the two analysed variants. The results have been analysed qualitatively and quantitatively, and the results of the analyses are included in the following chapters.

4.1. Integration variant I – tachymeter measurement

In the first integration variant, UAV images were processed based on GCPs, the coordinates of which were determined using the tacheometric method, with an error $mp_{XYZ} < 3$ mm. Such a high accuracy was possible due to the use of a precise total station and the establishment of a geodetic control network, which was adjusted. Three GCPs located around the church were used for georeferencing. The distribution of ground control points and check points on the background of a true high-resolution orthomosaic is presented in Figure 5.

The direction and size of the error ellipses presented in Figure 5 indicate the error of the horizontal components, while the colour of the ellipse indicates the error of the height component. The $RMSE_{XYZ}$ error at the check points was 1.5 cm, which is the value that corresponds to

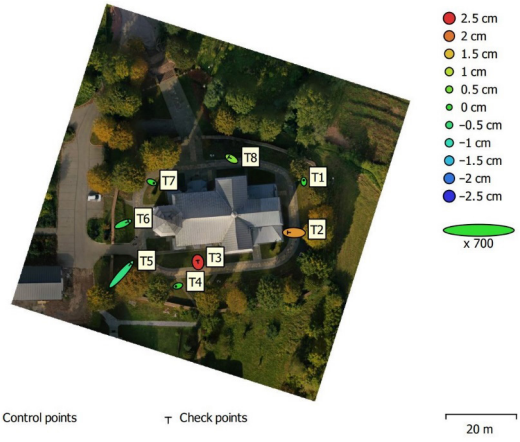

Figure 5. Distribution of control points and check points with their determination errors for the integration of UAV and TLS data based on tacheometer measurement (I variant)

the geometric mean resolution of the images acquired by the UAV. The point cloud generated from the UAV images was imported into Cloud Compare software. When the UAV point cloud was treated as a reference layer, it was merged with the TLS point cloud by indicating the three homologous points needed to determine the transformation matrix. A summary of the cloud matching deviations on homologous points is presented in Table 2.

Table 2. Summary of TLS to UAV point cloud matching deviations

Matching point number	Deviation of fit ΔXYZ [m]
T4-T4’	0.009
T6-T6’	0.013
T8-T8’	0.005

The mean deviation for the first analysis variant was 0.008 [m]. The results of data integration were accepted and merged as a single point cloud. Within the first variant of analyses, the point cloud contained coordinates recorded in the Polish large-scale geometry system (EPSG: 2178).

4.2. Integration variant II – measurement by scanner

For the second variant of data fusion, UAV images were subjected to absolute orientation based on GCPs measured by laser scanning alone. As in the previous case, 3 GCPs were used to provide georeferencing. The smaller number of check points in relation to the previous case resulted from the problem of scanning two signalled chequerboard control points (points T2 and T3). The model was fitted to the control points, while the error at the check points was $RMSE_{XYZ}$ = 1.9 cm. The distribution of errors for the second variant of the analyses is presented in Figure 6. Both error values are similar in the two analysed cases. Small error values testify to the high precision of the measurements of the indicated photogrammetric network. Thus,

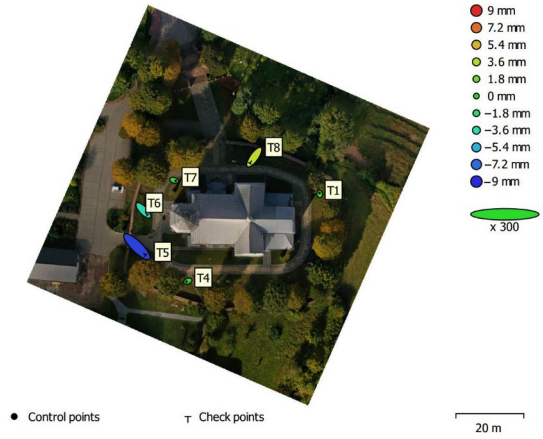

Figure 6. Distribution of control points and check points with their determination errors for the integration of UAV and TLS data based on scaner measurement (II variant)

the point cloud obtained from UAV images was exported for further calculations.

Within the second variant, a point cloud from laser scanning was treated as a reference layer, to which a point cloud from the UAV was matched. As in the previous stage, data integration was carried out on the basis of three homogeneous points, corresponding to the first variant of analysis: T4, T6, T8. The results of point cloud matching are presented in Table 3.

Table 3. Summary of UAV to TLS point cloud matching deviations

Matching point number	Deviation of fit ΔXYZ [m]
T4-T4’	0.022
T6-T6’	0.032
T8-T8’	0.015

The average deviation for the second analysis variant was 0.024 [m]. The resulting point cloud, after integration with UAV data, was stored in the local coordinate system of the scanner. At this stage, two-point clouds were obtained after integration of UAV and laser scanning data. They were the basis for the full reconstruction of the surface of the sacred object and the creation of 3D models.

4.3. Visual analysis of the generated 3D models

Using the methodology presented (Figure 4), two 3D models of the same religious building were generated. Model generation was carried out in an iterative manner until satisfactory visual effects were obtained. During mesh generation, an anomaly was observed on the church tower in the form of a pronounced bulge. The distorted element was highly overexposed in the UAV images, which could indicate noise that was not properly removed by filtering the integrated point clouds. Another reason for the incorrect modelling could have been insufficient batch data. To correct this error, it would be necessary to acquire another series of ground images at a different time of day. The tower bulge was manually corrected in Agisoft Metashape software. In the end, the resulting 3D models were similar in terms of visualising the various object details, which is related to the similar accuracy of point cloud generation from the UAV for both analysis variants. In addition, the same drone images were used for texturing at 8k resolution for both variants, which further justifies the visual convergence of the presented 3D models. Figure 7 presents a view of one of the created 3D models from different directions of the world.

In both Figures 7a and 7c, no locations on the object indicating 3D modelling errors were observed. In Figure 7b, an error was identified in the texture of the roof over the chapel. This may be due to the small number of UAV images on which this feature was mapped as a result of its being obscured by nearby trees. Despite the southern time of day during which the UAV images were acquired,

a) b) c)

Figure 7. Visualization of one of the two resulting 3D models of the sacred site: a – view from the southeast; b – view from the northwest; c – view from the east

shadows and partial loss of contrast could not be avoided. Nevertheless, the final modelling results were considered satisfactory and eligible for detailed accuracy analyses based on them.

4.4. Quantitative comparison of spatial data integration variants

To carry out a detailed analysis of the accuracy of the geometry of the resulting 3D models, the spatial coordinates of 10 architectural details on the site were acquired in the field. The coordinates were calculated in the local system and surveyed using the tacheometric method. For both generated 3D models, the coordinates of characteristic architectural details were read out and deviations between the coordinates from the 3D models and from the total station measurement were calculated. A summary of the results obtained is presented in Figure 8.

As a result of the control measurements, a mean square error of 1.7 cm was obtained for the first variant of the analyses and $RMSE_{XYZ}$ of 2.5 cm for the second variant of the work. The results obtained confirm that the quality of the 3D models is very close to each other. However, higher accuracies on the 3D model were obtained when the GCP measurement was done by tacheometry rather than laser scanning.

5. Discussion

Cultural heritage is a record of the human past and, as monuments, shows great diversity in terms of geometric complexity or the nature of its origin. Monuments are affected by damage attracted by the impact of erosion, past wars, natural disasters or human neglect. According to Escarcena et al. (2011), a monument can only be restored and protected if it has been fully measured and documented and its development is successively monitored.

The selection of an appropriate technique for the creation of digital documentation of cultural heritage objects is difficult and involves the analysis of many work steps such as: the choice of data acquisition methods, optimal workflow, and obtaining a product compliant with the requirements of technical specifications and national standards. For the object analysed in this paper, it would not have been possible to obtain full information on the geometry of the tower and the roof had it not been for the point cloud generated from the UAV images (Figure 4). Aerial images additionally made it possible to assess the condition of the roof and decide on the roof renovation.

The combination of TLS scanning methods and close-range photogrammetry allows one to streamline and optimise the cultural heritage documentation process. UAV imagery and point clouds from TLS can, according to

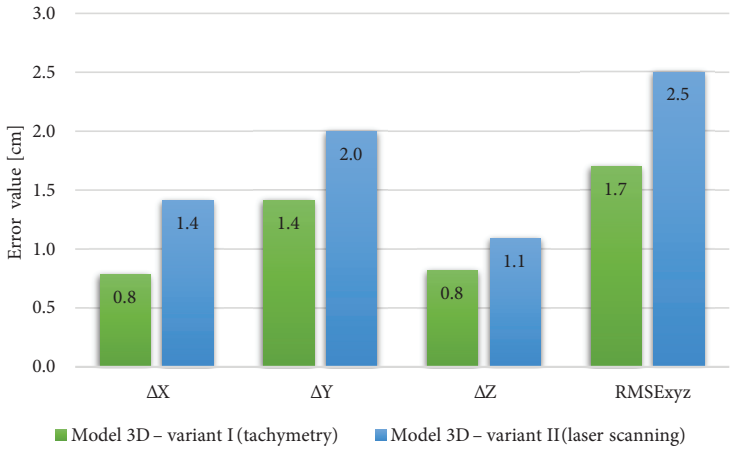

Figure 8. Summary of deviations and errors at check points for two analysis variants and obtained 3D models

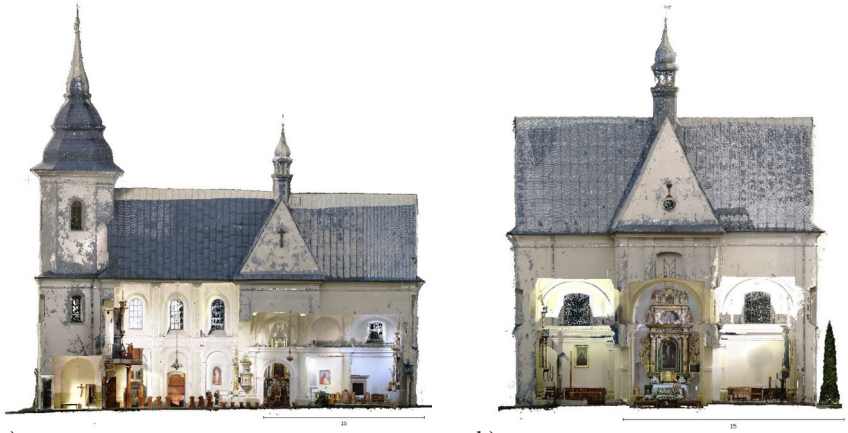

a) b)

Figure 9. Cross-section through the point cloud after UAV and TLS data integration: a – view of the north elevation of the church; b – view of the east elevation of the church and the altar

Escarcena et al. (2011), be complementary, and the disadvantages of one system can be compensated for by the advantages of the other. TLS allows for high spatial reliability and detail of the collected information, while techniques based on digital images allow obtaining valuable information for correct point cloud interpretation. In this work, without the integration of UAV and TLS data, it would be impossible to create a complete 3D model (Figure 7) or to generate any cross-section through the point cloud (Figure 9).

Both TLS and UAV measurements are dependent on meteorological conditions (precipitation, humidity, sunshine), which means that the planning of measurements using the presented methods should be done in a thoughtful and precise way. In case of large overexposure or underexposure on the images, the authors of this article recommend taking additional series of ground images at a different time of the day. The problem of overexposure of the images for a fragment of the tower caused incorrect generation of the mesh grid and reconstruction of the tower geometry, which required manual correction of the errors (Figure 4b).

The generated two-point clouds from the UAV images were similar in terms of accuracy of fitting into the check points, which is confirmed in Figure 5 and Figure 6. This means that having a laser scanner of Faro Focus 150S class, there is no need to measure the control points with the tachymetry method if the measurement accuracy ordered by the Ordering Party is no higher than 2 cm. This is further confirmed in Figure 8 and the error of combining point clouds obtained from different sensors at the control points on the site. Measurement of ground control points with the TLS method allows for streamlining the measurement process and reducing the number of people involved in the field work to one person. Visual analysis of the resulting 3D models (Figure 7) did not show any significant errors during triangulation and texturing. The detailed accuracy analysis presented in Figure 8 confirmed the cartometricity of the resulting spatial models in the full 3D dimension and the possibility of measuring selected elements of the object with an accuracy of less than 3 cm. This means that the resulting 3D models are suitable for conducting measurements for the inventory of the presented church. The innovation of the research presented in this paper is the demonstration that the use of the TLS scanner in the creation of consistent point clouds with the data obtained from the UAV method allows the final results to be obtained with a very good accuracy, as demonstrated by comparison with the geodetic network established with the tachymeter.

Conclusions

The development of close-range photogrammetry in recent years has significantly expanded the possibility of creating technical building documentation and collecting aerial information on a larger scale (Kapica et al., 2013; Mikrut et al., 2013). The photogrammetric point cloud allows to improve the quality of the 3D model by completing data for the upper parts of the building, which are difficult to obtain by laser scanning. Integrated 3D models have great potential to document heritage sites, manage them intelligently, and take preventive measures for conservation (Jo & Hong, 2019).

Taking into account factors such as accuracy, cost, time of fieldwork conducted, and the resulting 3D model output, the authors of this study assess the technologies used as efficient and conducive to conducting inventories of cultural heritage sites. In the course of the work carried out, the TLS method was positively evaluated as a GCP measurement technique for the integration of UAV and TLS data and the creation of accurate 3D models of large-scale religious buildings.

Acknowledgements

The authors would like to thank Priest Stanisław Malec for making the object available for research and for his valuable comments during the work carried out.

References

Bieda, A., Bydłosz, J., Warchoł, A., & Balawejder, M. (2020). Historical underground structures as 3D cadastral objects. *Remote Sensing*, *12*(10). https://doi.org/10.3390/rs12101547

Chow, J. C. K. (2014). *Multi-sensor integration for indoor 3D reconstruction* [PhD Thesis, University of Calgary] (pp. 37–76).

Cienciała, A. (2018). *Selected issues concerning management of historical immovable properties in Poland and other European countries* [Conference presentation]. Geographic Information Systems Conference and Exhibition "GIS ODYSSEY 2018", Italy, Perugia.

Cox, R. P. (2015). *Real-world comparisons between target-based and targetless point-cloud registration in FARO Scene, Trimble RealWorks and Autodesk Recap* [PhD Thesis, University of Southern Queensland].

Escarcena, J .C., De Castro, E. M., García, J. L. P., Calvache, A. M., Del Castillo, T. F., García, J. D., Cámara, M. U., & Castillo, J. C. (2011). Integration of photogrammetric and terrestrial laser scanning techniques for heritage documentation. *Virtual Archaeology Review*, 2(53), 53–57. https://doi.org/10.4995/var.2011.4605

Esmer, M., Kudumović, L., & Kasmo, R. (2019). A case study of terrestrial laser scanning for urban conservation studio at Çarşamba Neighbourhood in Istanbul. *Polytechnic & Design*, *7*(3), 211–218.

Federman, A., Shrestha, S., Quintero, M. S., Mezzino, D., Gregg, J., Kretz, S., & Ouimet, C. (2018). Unmanned Aerial Vehicles (UAV) photogrammetry in the conservation of historic places: Carleton immersive media studio case studies. *Drones*, *2*(2), 18. https://doi.org/10.3390/drones2020018

FARO. (n.d.). *User manual guide. Faro Focus 150 S.* Retreived May 8, 2022 from https://knowledge.faro.com/Hardware/3D_Scanners/Focus/User_Manuals_and_Quick_Start_Guides_for_the_Focus_Laser_Scanner

Gbopa, A. O., Ayodele, E. G., Okolie, C. J., Ajayi, A. O., & Iheaturu, C. J. (2021). Unmanned aerial vehicles for three-dimensional mapping and change detection analysis. *Geomatics and Environmental Engineering*, *15*(1), 41–61. https://doi.org/10.7494/geom.2021.15.1.41

Gradka, R., Majdańska, R., & Kwinta, A. (2019). Example of historic building inventory with an application of UAV photogrammetry. *Geomatics, Landmanagement and Landscape*, (4), 201–217. https://doi.org/10.15576/GLL/2019.4.201

Granek, G., Toś, C., & Wolski, B. (2020). Implementation of virtual reference points in registering scanning images of tall structures. *Open Geosciences*, *12*(1), 876–886. https://doi.org/10.1515/geo-2020-0131

Hejmanowska, B., Głowienka, E., Michałowska, K., Mikrut, S., Kramarczyk, P., Opaliński, P., & Struś, A. (2017, June 22–25). 4D reconstruction and visualisation of Krakow Fortress. In *Proceedings of the 2017 Baltic Geodetic Congress (BGC Geomatics)*, Gdansk, Poland (pp. 1–5). IEEE. https://doi.org/10.1109/BGC.Geomatics.2017.83

Hlotov, V., & Marusazh, K. H. (2019). Accuracy investigation of point Cloud with Faro Focus 3D S120 terrestrial laser scanner. *Geodesy, Cartography and Aerial Photography*, *90*. https://doi.org/10.23939/istcgcap2019.90.041

Jo, Y. H., & Hong, S. (2019). Three-dimensional digital documentation of cultural heritage site based on the convergence of terrestrial laser scanning and unmanned aerial vehicle photogrammetry. *ISPRS International Journal of Geo-Information*, *8*(2), 53. https://doi.org/10.3390/ijgi8020053

Kapica, R., Vrublová, D., & Michalusová, M. (2013). Photogrammetric documentation of Czechoslovak border fortifications at Hlučín-Darkovičky. *Journal of Geodesy and Cartography*, *39*(2), 72–79. https://doi.org/10.3846/20296991.2013.806243

Karabin, M., Bakuła, K., & Łuczyński, R. (2021). Verification of the geometrical representation of buildings in cadastre using UAV photogrammetry. *Geomatics and Environmental Engineering*, *15*(4), 81–99. https://doi.org/10.7494/geom.2021.15.4.81

Kowalska, M., & Zaczek-Peplinska, J. (2018). Examples of measuring marks used in geo-reference and the connection between classic geodetic measurements and terrestrial laser scanning. *Technical Transactions*, *1*, 151–162.

Liang, H., Li, W., Lai, S., Zhu, L., Jiang, W., & Zhang, Q. (2018). The integration of terrestrial laser scanning and terrestrial and unmanned aerial vehicle digital photogrammetry for the documentation of Chinese classical gardens – A case study of Huanxiu Shanzhuang, Suzhou, China. *Journal of Cultural Heritage*, *33*, 222–230. https://doi.org/10.1016/j.culher.2018.03.004

Lipiceki, T., Jaśkowski, W., Matwij, W., & Skobliński, W. (2017). Zastosowanie skanera Faro Focus X330 w ocenie pionowości komina o wysokości 220 m. *Przegląd Górniczy*, *6*, 44–53 (in Polish).

Mikoláš, M., Jadviščok, P., & Molčák, V. (2014). Application of terrestrial photogrammetry to the creation of a 3D model of the Saint Hedwig Chapel in the Kaňovice. *Geodesy and Cartography*, *40*(1), 8–13. https://doi.org/10.3846/20296991.2014.906923

Mikrut, S., Głowienka-Mikrut, E., & Michałowska, K. (2013). The UAV technology as a future-oriented direction in the development of low-ceiling aerial photogrammetry. *Geomatics and Environmental Engineering*, *7*(4), 69–77. https://doi.org/10.7494/geom.2013.7.4.69

Puniach, E., Bieda, A., Ćwiąkała, P., Kwartnik-Pruc, A., & Parzych, P. (2018). Use of Unmanned Aerial Vehicles (UAVs) for updating farmland cadastral data in areas subject to landslides. *ISPRS International Journal of Geo-Information*, *7*(8). https://doi.org/10.3390/ijgi7080331

Pyka, K., Wiącek, P., & Guzik, M. (2020). Surveying with photogrammetric unmanned aerial vehicles. *Archives of Photogrammetry, Cartography and Remote Sensing*, *32*, 79–102.

Ramondino, F. (2011). Heritage recording and 3D modeling with photogrammetry and 3D scanning. *Remote Sensing*, *3*, 1104–1138. https://doi.org/10.3390/rs3061104

Reiss, M. L. L., Da Rocha, R. S., Ferraz, R. S., Cruz, V. C., Morador, L. Q., Yamawaki, M. K., Rodrigues, E. L. S., Cole, J. O., & Mezzomo, W. (2016). Data integration acquired from micro-UAV and terrestrial laser scaner for the 3D mapping of jesuit ruins of Sao Miguel Das Missoes. *The International Archives of the Photogrammetry, Remote Sensing and Spatial Information Sciences*, *XLI-B5*, 315–321. https://doi.org/10.5194/isprs-archives-XLI-B5-315-2016

Reshetyuk, Y. (2009). *Terrestrial laser scanning: Error sources, self-calibration direct georeferencing*. VDM Verlag.

Róg, M., & Rzonca, A. (2021). The impact of photo overlap, the number of control points and the method of camera calibration on the accuracy of 3D model reconstruction. *Geomatics and Environmental Engineering*, *15*(2), 67–87. https://doi.org/10.7494/geom.2021.15.2.67

Šašak, J., Gallay, M., Kaňuk, J., Hofierka, J., & Minár, J. (2019). Combined use of terrestrial laser scanning and UAV photogrammetry in mapping alpine terrain. *Remote Sensing*, *11*(18). https://doi.org/10.3390/rs11182154

Sobura, S. (2022). Calibration of the low-cost UAV camera on a spatial test field. *Geodesy and Cartography*, *48*(3), 134–143. https://doi.org/10.3846/gac.2022.16215

Sztubecki, J., Bujarkiewicz, A., Derejczyk, K., & Przytuła, M. (2018). A hybrid method of determining – deformations of engineering structures with a laser station and a 3d scanner. *Civil and Environmental Engineering Reports*, *28*, 277–185. https://doi.org/10.2478/ceer-2018-0028

Tokarczyk, R., Kohut P., Mikrut, S., & Kolecki, J. (2012). Review of methods of texturing 3D object models obtained through terrestrial laser scanning and photogrammetric techniques. *Archiwum Fotogrametrii, Kartografii I Teledetekcji*, *24*, 367–381.

Xu, Z., Wu, L., Shen, Y., Li, F., Wang, Q., & Wang, R. (2014). Tridimensional reconstruction applied to cultural heritage with the use of camera-equipped UAV and terrestrial laser scanner. *Remote Sensing*, *6*(11). https://doi.org/10.3390/rs61110413

Zespół kościoła parafialnego pw. św. Marii Magdaleny i św. Mikołaja. (n.d.). Retrieved February 20, 2022, from https://zabytek.pl/pl/obiekty/chelmce-zespol-kosciola-par-pw-sw-marii-magdaleny-i-sw-mikol